



UNIVERSITY OF LEEDS

This is a repository copy of *Improved conversion of residual MSW biomass waste to sugars using online process monitoring and integrated contamination control*.

White Rose Research Online URL for this paper:

<https://eprints.whiterose.ac.uk/168608/>

Version: Accepted Version

Article:

Barba, FC, Chacón, MG, Reynolds, WR et al. (3 more authors) (2021) Improved conversion of residual MSW biomass waste to sugars using online process monitoring and integrated contamination control. *Bioresource Technology Reports*, 13. 100612. ISSN 2589-014X

<https://doi.org/10.1016/j.biteb.2020.100612>

© 2020 Published by Elsevier. Licensed under the Creative Commons Attribution-NonCommercial-NoDerivatives 4.0 International License (<http://creativecommons.org/licenses/by-nc-nd/4.0/>).

Reuse

This article is distributed under the terms of the Creative Commons Attribution-NonCommercial-NoDerivatives (CC BY-NC-ND) licence. This licence only allows you to download this work and share it with others as long as you credit the authors, but you can't change the article in any way or use it commercially. More information and the full terms of the licence here: <https://creativecommons.org/licenses/>

Takedown

If you consider content in White Rose Research Online to be in breach of UK law, please notify us by emailing eprints@whiterose.ac.uk including the URL of the record and the reason for the withdrawal request.



eprints@whiterose.ac.uk
<https://eprints.whiterose.ac.uk/>

1 **Improved conversion of residual MSW biomass waste to sugars using online process**
2 **monitoring and integrated contamination control**

3 Fernando Climent Barba^{ab}, Micaela G. Chacón,^b William R. Reynolds^b, Dhivya J. Puri^c
4 Richard A. Bourne^{b*}, A. John Blacker^b

5 ^aCentre for Doctoral Training in Bioenergy, School of Chemical and Process Engineering,
6 University of Leeds, LS2 9JT, United Kingdom

7 ^bInstitute of Process Research and Development, School of Chemistry and School of
8 Chemical and Process Engineering, University of Leeds, LS2 9JT, United Kingdom

9 ^cFiberight Ltd., Research and Development, Unit 73 Basepoint Enterprise Centre,
10 Southampton SO14 5FE

11 **Correspondence:** Dr Richard A. Bourne, School of Chemical and Process Engineering,
12 University of Leeds, Woodhouse Lane, Leeds, LS2 9JT, UK

13 **E-mail:** R.A.Bourne@leeds.ac.uk

14 **Abstract**

15 Enzymatic saccharification of lignocellulosic biomass to soluble sugars is vulnerable to
16 microbial contamination. Identification of early stage indicators of contamination could
17 allow for more rapid intervention and improved sugar retention. Here we validate the use
18 of dissolved oxygen (DO) and pH as early-stage indicators, and used to evaluate the
19 effectiveness of several antimicrobial agents (sodium azide, benzisothiazolinone,
20 hydrogen peroxide and tetracycline). It was found that benzisothiazolinone (BIT) and
21 sodium azide performed most favourably (8.93 and 9.89 g glucose/L, respectively),

22 controlling contamination for the entire 24 hour time course assessed. We then describe
23 the development of a novel integrated control system with online monitoring of DO/pH
24 and automatic administration of a discrete doses of antimicrobial agent to the reaction
25 once environmental DO dropped below a pre-defined threshold. Further, we show that
26 FTIR can be used for continuous real-time glucose quantification during enzyme
27 hydrolysis as an alternative to traditional offline measurement methods.

28 **Keywords:** Municipal solid waste (MSW); Enzymatic hydrolysis; Microbial growth
29 indicators; Antimicrobial agents; Process monitoring

30 **1 Introduction**

31 Lignocellulosic biomass, which includes materials such as forestry residue, agricultural
32 residue, the organic fraction of municipal solid waste (OFMSW), etc., is an attractive
33 feedstock for biorefineries due to its low cost and widespread availability (Hazar, 2013;
34 Jönsson and Martín, 2016) The hydrolysis of the carbohydrate fraction of lignocellulosic
35 biomass into its constitutive pentose and hexose sugars is of primary interest as they can
36 be further transformed into value-added products (e.g. ethanol, lactic acid or butanol) via
37 chemical conversion or microbial fermentation (Puri et al., 2013; Sluiter et al., 2012). One
38 of the least exploited sources of lignocellulosic biomass is municipal solid waste (MSW),
39 despite it being produced in great quantities worldwide (Jensen et al., 2010). While it
40 varies by region, the lignocellulosic fraction of OFMSW is estimated to be ~30%, of
41 which a significant proportion is composed of plant-derived carbohydrates, making this
42 a viable source of non-food sugar (Hazar, 2013; Meor Hussin et al., 2013).

43 The conversion of lignocellulose to monosaccharides is typically achieved via a two-step
44 process involving an initial pretreatment followed by an enzyme hydrolysis. The role of

45 the pretreatment step is to upset the natively recalcitrant structure of the biomass and clear
46 away any physical and chemical barriers which render the cellulose less accessible to
47 relevant downstream enzymes (Hendriks and Zeeman, 2009; Jönsson and Martín, 2016;
48 Wahlström and Suurnäkki, 2015). A number of pretreatment regimes are currently in use,
49 and can be broadly classified as: chemical, physical, biological and physiochemical
50 (Bhatia et al., 2020). A large draw back to a number of pretreatment strategies, however,
51 is the generation of degradation products, which are inhibitory to the downstream
52 hydrolysis step. As such, the development of methods to alleviate any pretreatment
53 inhibition issues is an active field of research (Hassan et al., 2018; Jönsson and Martín,
54 2016). While the secondary hydrolysis step can be carried out either enzymatically or via
55 acid hydrolysis, the former is widely preferred as it offers high selectivity while being a
56 more environmentally benign process (Wahlström and Suurnäkki, 2015). Enzyme
57 hydrolysis is carried out by a cocktail of enzymes working synergistically to deconstruct
58 the lignocellulose. A wealth of work has been carried out to design optimal combinations
59 and ratios of those enzymes present within these cocktails – including but not limited to
60 endoglucanases, cellobiohydrolases, and β -glucosidases, lytic polysaccharide mono-
61 oxygenases (LPMOs), etc. – to maximize hydrolysis for different biomass substrates
62 subjected to different pretreatments (Van Dyk and Pletschke, 2012; Wahlström and
63 Suurnäkki, 2015). However, enzymatic saccharification continues to suffer some techno-
64 economic barriers; including biomass recalcitrance, enzyme costs, end-product
65 inhibition, and low volumetric production compared to food-based sugars (Jönsson and
66 Martín, 2016). Importantly, achieving an economically successful hydrolysis process will
67 require not only improving sugar productivity, but also improving sugar retention.

68 With the enzymatic hydrolysis of lignocellulosic material resulting in the accumulation
69 of its constitutive monomeric sugars, this step is vulnerable to microbial contamination.
70 Glucose is the primary fuel for microbes, providing the energy required for cell growth
71 and proliferation (Johnston, 1999). As such, any microbial contamination can lead to a
72 significant loss in sugar titres. Preventative measure intended at minimizing the risk of
73 contamination can be carried out prior to enzyme hydrolysis; which could include
74 sterilization of hydrolysis equipment and/or the inclusion of an additional autoclave step
75 to sterilize the lignocellulosic feedstock (Schell et al., 2007; Serate et al., 2015). Both
76 practices possess drawbacks, with the former not always being sufficient to eliminate
77 contamination, and the latter running the risk of generating unwanted inhibitors, as well
78 as increasing the overall time and process cost of a large-scale operation (Hassan et al.,
79 2018). Alternatively, the use of antimicrobial agents during the enzyme hydrolysis can be
80 very effective at controlling contamination. However, a number of considerations need to
81 be made when selecting such an agent, such as: (1) the mode of action of the agent, (2)
82 its short and long term stability in solution, (3) the fate of the sugar rich hydrolysate (i.e.
83 fermentation or chemical conversion), and (4) minimizing the potential of developing
84 antibiotic resistant bacterial strains (Gandla et al., 2018; Islam et al., 1999; Serate et al.,
85 2015). Currently, biological contamination is primarily diagnosed through the detection
86 of organic acids, such as lactic acid, in the sugar rich hydrolysate (Rich et al., 2020).
87 These acids are the end-product of anaerobic fermentation pathways and are therefore
88 indicators of contamination once detected (Serate et al., 2015). Earlier diagnosis could
89 instead be achieved by *in situ* monitoring of upstream environmental indicators of
90 microbial growth and fermentation, specifically, dissolved oxygen (DO) and pH. With
91 oxygen being required for cellular respiration, its consumption increases concomitantly

92 with microbial population density (Garcia-Ochoa et al., 2010; Riedel et al., 2013). In the
93 absence of constant replenishment, microbial oxygen demand will eventually exceed
94 dissolved oxygen availability, resulting in its depletion. In the absence of oxygen, a
95 number of microbial species will metabolically switch to anaerobic fermentation for
96 energy synthesis, the product(s) of which are short chain alcohols and acids (Ward, 2014).
97 Consequently, the accumulation of these products results in a drop in environmental pH.
98 Thus, an observed drop in environmental DO followed by a drop in pH is a classic
99 indication of microbial growth and fermentation (Deepak et al., 2008; Famelart et al.,
100 1987).

101 Generally, enzyme hydrolyses are poorly monitored over the course of the reaction, with
102 sugar and acid quantification being carried out intermittently by offline methods such as
103 HPLC and enzyme assay, while DO and pH are rarely tracked (Gandla et al., 2018).
104 Herein, we validate the use of DO and pH as metrics for the diagnosis of early stage
105 microbial contamination during enzymatic hydrolysis of MSW pulp, and use them to
106 evaluate the effectiveness of a number of antimicrobial agents (sodium azide,
107 benzisothiazolinone, hydrogen peroxide, and tetracycline). We then demonstrate the use
108 of an integrated control system with continuous process monitoring of DO and pH and a
109 custom-made operating system designed to automatically issue a defined dose of a given
110 antimicrobial agent once environmental DO has dropped below a pre-set threshold.
111 Further, we show here the first use of *in situ* FTIR for real-time sugar quantification
112 during lignocellulosic biomass hydrolysis as an alternative to the more commonly used
113 offline techniques, such as HPLC and enzyme assays. This work lays the foundation for
114 entirely online monitoring of enzymatic hydrolysis reactions, the application of which
115 could improve both sugar production and sugar retention.

116 **2 Materials and Methods**

117 Cellic[®] CTec3 was kindly donated by Novozymes (Copenhagen, Denmark) and
118 Fermasure[®] was purchased from Dupont, Ltd. (London, UK). All other chemicals and
119 reagents were purchased from Sigma Aldrich (Dorset, UK) or Fisher Scientific
120 (Loughborough, UK) unless stated otherwise.

121 MSW pulp was provided by Fiberight Ltd. from its pilot plant in Lawrenceville (Virginia,
122 USA). Plastics and metals were removed and the lignocellulosic fraction (consisting of
123 mostly paper and card) was pulped by a series of hydrothermal processes. The resulting
124 fibrous material was supplied at a dry matter of 50-55%, parameter determined by the
125 “oven-drying method”. The lignocellulose composition was determined to be 55%
126 glucan, 12% xylan, 6% araban/galactan/mannan, 24% lignin, 3% ash (Puri et al., 2013).

127 *2.1 Enzymatic hydrolysis of MSW pulp*

128 Enzymatic hydrolysis was carried out in a 1 L jacketed-vessel (Scientific UK) for 24
129 hours at 50 °C, agitated with a 4 pitched-blade impeller (Caframo Limited, Ontario,
130 Canada) at 700 rpm. Hydrolysis reactions were carried out using either 6% or 7% total
131 solids (TS, %) of MSW pulp and 2% (w/w dry substrate) CTec3 enzyme cocktail in a
132 reaction medium of water, totalling a working mass of 800 g. Slurry pH was adjusted to
133 5.25 using 6% phosphoric acid and was then incubated at 50 °C for 30 minutes prior to
134 the addition of enzyme. 0.1% (w/w dry substrate) of either NaN₃ (sodium azide), BIT
135 (benzisothiazolinone), H₂O₂ (hydrogen peroxide) or , tetracycline were added to the
136 reaction slurry immediately prior to the addition of CTec3 at the beginning of the reaction,
137 or once DO reached 0 mg/L (typically at hour 6). For those reactions, antimicrobial agent

138 was added once the DO had reached 0 mg/L, slurry pH was adjusted using 10 % sodium
139 hydroxide if it dropped below 4.75 for the first 8 hours.

140 Samples from the hydrolysis slurry were withdrawn from a well-mixed region close to
141 the impeller and centrifuged at 4000 rpm for 15 minutes. The hydrolysate was then passed
142 through a 0.45 µm filter and stored frozen at -20 °C until analysis.

143 2.2 Integrated control system

144 To prevent the growth of microorganisms in the sugar-rich reaction mass, an integrated
145 control system was designed with three main sub-systems: (1) process monitoring, (2)
146 operating system, (3) automatic dosing system. A schematic of this set up is shown in
147 Fig. S1. During enzymatic hydrolysis, the pH and DO were measured with the
148 corresponding sensors: InLaB® probes (previously calibrated with vendor standards)
149 installed in the SevenExcellence™ multi-parameter kit. Continuous recordings (1 minute
150 frequency) were automatically transferred to, Labx direct pH 3.3 (Mettler Toledo, USA)
151 monitoring software, generating *.txt files*. A bespoke operating system, named “*glucose*
152 *bioreactor model*”, was programmed using LabVIEW (National Instruments, UK)
153 (Blacker et al., 2019) This incorporates on-line data and commands the automatic dosing
154 of anti-microbial agents by a syringe-pump unit (model 11, Harvard apparatus UK)
155 according to pre-defined settings (SI, Fig.S2) whereby a DO gradient threshold (ΔDO) is
156 set as an “alarm” for triggering the sterilising product: $\Delta DO < - 0.028 \text{ mg L}^{-1} \text{ s}^{-1}$. The
157 algorithm calculates the DO gradient according to the equation shown below. A full
158 description of the *glucose bioreactor model* can be found in the (SI, Fig.S2).

$$159 \quad \Delta D = \frac{DO_F - DO_{f'}}{f} \quad (Eq. 1)$$

160 Where: DO_F is the last monitored DO reading (mg/L), DO_{F-1} the value prior DO_F (mg/L)
161 and f is the frequency of monitoring (in s, e.g. 10 s).

162 2.3 Quantification of microbial population

163 Samples of slurry were taken at discrete time points during a hydrolysis reaction and
164 plated at several dilutions on Luria Broth agar plates (10 g/L tryptone, 10 g/L NaCl, 5 g/L
165 yeast extract, 15 g/L agar). Plated samples were incubated at 50 °C for 16 hours.
166 Following incubation, colony forming units (CFUs) were counted and dilution corrected.

167 2.4 Quantification of products

168 Monomeric sugar and acid concentrations were quantified by HPLC. Monosaccharides
169 (D-glucose and D-xylose) and organic acids (L-lactic acid and acetic acid) were analysed
170 simultaneously by HPLC fitted with an Ultimate™ Dionex 3000, UK column. A 10 µL
171 sample was injected and separated by a Supelcogel™ C-610H (6% Crosslinked) column
172 with a deashing guard column, operating at 30 °C with 0.1 wt% phosphoric acid at a flow
173 rate of 0.5 ml.min⁻¹ as mobile phase. Monosaccharides and organic acids were detected
174 respectively by a Shodex RI-101 refractive index and a diode array detector (Thermo
175 Scientific, UK). High-purity analytical standards used to calibrate each product to
176 determine linear response concentrations. All samples were run in duplicate and
177 chromatograms were processed by Chromoleon software®.

178 On-line sugar analysis was performed by *in-situ* FTIR, monitoring sugar formation using
179 a MB3000 FTIR instrument (ABB, Switzerland). As glucose has an absorption peak at a
180 wavelength of 1035 cm⁻¹, a calibration curve was created by plotting absorbance at
181 1035cm⁻¹ relative to 0-100 g/L glucose concentration (SI, Fig.S3). After calibration, the
182 probe was fitted in a 2-L stirred tank reactor to monitor an enzymatic saccharification,

183 with absorbance (at 1035 cm^{-1}) readings taken every 120s by averaging 3 scans. FTIR
184 values were translated into g/L by the above-mentioned calibration curve in order
185 compare them with HPLC ones of given samples.

186 **3 Results and Discussion**

187 *3.1 Determining microbial contamination via pH/DO monitoring*

188 Both pH and DO are closely monitored and controlled during microbial fermentations in
189 order to optimize growth and productivity (Famelart et al., 1987; Jones et al., 1992;
190 Mohd-Zaki et al., 2016). Despite this, they are rarely used as metrics during enzyme
191 hydrolysis to evaluate the presence of microbial contamination. To validate that DO and
192 pH can be used as diagnostic tools for the detection of microbial contamination during
193 enzymatic hydrolysis of lignocellulose, a saccharification control reaction was run using
194 6% MSW pulp and 2% C-Tec3 enzyme cocktail. No pre-hydrolysis pulp sterilization
195 measures were taken nor any antimicrobial agents used, ensuring that the untreated pulp
196 was microbially compromised. This was confirmed as samples taken from said pulp
197 showed a mixed population of bacteria (SI, Fig. S4). During this reaction, it was found
198 that DO fluctuated for approximately the first 2 hours as the rheology of the slurry
199 changed due to the rapid initial activity of cellulases/endoglucanases, resulting in the
200 release of air from within the porous MSW matrix. During the first several hours, the
201 microbial population proliferated as DO and glucose were in abundance – the latter being
202 continuously released from the lignocellulose substrate (Fig. 1a-c). However, as there was
203 no continuous oxygen supplementation into the reaction mixture, eventually population
204 density reached a threshold whereby microbial oxygen demand exceeded its availability
205 (Fig. 2c). This resulted in a steep drop in DO by hour 5.5, with 0 mg/L being reached by

206 hour 6 (Fig. 1a). At this point, the environmental pH began to drop as those species
207 capable of fermentation began to produce short chain acids. An analysis of reaction
208 products over the 24 hour time course showed that lactic acid began to accumulate
209 between hours 4-8 (Fig. 1b) and continued to do so over the course of the reaction,
210 culminating in a final titre of 140 mg/L at hour 24. The onset of lactic acid production
211 correlates well with the observed drop in environmental pH of the reaction, between hours
212 6-8. Lactic acid is a common product of microbial fermentation induced by anaerobic
213 conditions (Othman et al., 2017), and its presence is widely considered a symptom of
214 contamination (Serate et al., 2015). Unlike lactic acid, acetic acid was detected within
215 two hours of the start of the reaction and continued to increase slowly over the 24-hour
216 time course to a final concentration of 60 mg/L (Fig. 1b). While acetic acid can also be a
217 fermentation product from a number of microbial species (Raspor and Goranovič, 2008),
218 it is also released upon the hydrolysis of acetyl groups from hemicellulose during
219 saccharification (Jönsson and Martín, 2016; Serate et al., 2015)). Thus, unlike lactic acid,
220 it is not a definitive indicator of microbial contamination. Final glucose titres did not
221 change between hours 8-24 (Fig. 1b) which would suggest that glucose production and
222 glucose utilization – either through microbial fermentation to lactic acid or biomass
223 accumulation – are in equilibrium.

224 Having confirmed that a drop in environmental DO and pH during the enzymatic
225 hydrolysis of lignocellulose is correlated with the early growth phase of a microbial
226 population, we used this criterion to time the application of an antimicrobial dose into the
227 reaction mixture in order to halt microbial proliferation and improve glucose yield (Fig.
228 2a-c). The hydrolysis was carried out under the same conditions as described above, with
229 the exception that once DO reached 0 mg/L, just before hour 6, 0.1% (w/w dry substrate)

230 BIT, a bactericidal antimicrobial, was manually injected into the slurry. Nearly
231 immediately, the DO rose to 5 mg/L, and an analysis of CFUs present within the slurry
232 at hour 8 showed a significant reduction in population density, with a further drop by hour
233 24 (Fig. 2c). It has previously been found that during microbial death phase, that dissolved
234 oxygen increases as its overall consumption is reduced – explaining this observed pattern
235 (Riedel et al., 2013). Further, it was found that pH, which had begun to drop slightly
236 following the early state of DO exhaustion, also stabilized after the addition of the
237 antimicrobial dose (Fig. 2a). While this would suggest fermentation had begun prior to
238 the BIT addition, no lactic acid was detected throughout the time course. Conversely,
239 acetic acid production was observed from hour 2 onwards. Further, unlike the control
240 reaction which had no antimicrobial supplementation, glucose titres continued to rise
241 between 8-24 hours, resulting in a final titre of 9.5 g/L for the reaction in which BIT was
242 added. While presumably a small amount glucose will have been converted to microbial
243 biomass prior to the BIT addition, this still represents a 40% improvement in glucose
244 production compared to the no antimicrobial control.

245 Ultimately, monitoring DO and pH over the course of an enzymatic hydrolysis of
246 lignocellulose represents a strategy that is easy to implement and could allow for earlier
247 detection of microbial contamination compared to the more commonly used downstream
248 indicator, such as the accumulation of short chain acids (Serate et al., 2015). Potentially
249 enabling faster intervention and therefore maximization of sugar production. This is
250 especially useful for large industrial-scale monomeric sugar production where pre-
251 sterilization of pulp via autoclave may be unrealistic due to the high capital and operating
252 costs, while pasteurization of hydrolysis equipment is not always effective at eliminating
253 contamination (Rich et al., 2020; Serate et al., 2015). Further, the continuous monitoring

254 of DO and pH during the hydrolysis of lignocellulose can have the additional benefit of
255 ensuring consistently optimal conditions for the protein mediated saccharification. Those
256 enzymes present within the majority of commercial cocktails work optimally within a
257 specific pH range, while the recent discovery of lytic polysaccharide monooxygenase
258 enzymes and their utilization of molecular oxygen as a co-substrate highlights the need
259 to closely control both these factors (Du et al., 2012; Fenila and Shastri, 2016; Gusakov
260 et al., 2017).

261 *3.2 Tackling microbial contamination by several antimicrobial agents according to* 262 *pH/DO metrics*

263 With MSW pulp typically containing a mixed microbial population of bacteria, yeast and
264 fungal species (Hassen et al., 2001) the selection of an antimicrobial agent with broad
265 spectrum activity becomes highly important. Following on from the results with BIT in
266 Section 3.1, we sought to demonstrate the application of DO and pH as metrics to evaluate
267 the efficacy of a number of other commonly used antimicrobial agents to control the
268 proliferation of a mixed microbial population during the enzymatic hydrolysis of
269 unsterilized MSW pulp. To test this, MSW saccharification time courses were run as
270 described in section 3.1, where once DO reached 0 mg/L, a 0.1% (w/w dry substrate) dose
271 of either: sodium azide (NaN_3), hydrogen peroxide (H_2O_2) or tetracycline was manually
272 injected into the slurry, and pH, DO, monomeric sugars, and organic acids were
273 monitored for 24 hours (Fig. 3a-f). A comparison of each time course demonstrated that
274 a drop in the measured values for both DO and pH were good indicators of infection and
275 correlated well with microbial viability as determined by the number of CFU/ml (Fig. 5).
276 Of the four antimicrobials tested, the most effective were BIT (Fig. 2a-c) and NaN_3 (Fig.

277 3a-c), while H₂O₂ and tetracycline were found to be insufficient at managing microbial
278 population over a 24 hour hydrolysis (Fig. 3c-f). This trend was additionally observed in
279 experiments where the antimicrobial dose was added at the onset of hydrolysis (Fig. S7a-
280 f).

281 The mode of action of NaN₃ is to inhibit the respiratory chain of gram-negative bacteria,
282 acting as a bacteriostat (Cabrol et al., 2017; Russo et al., 2008). Fig. 5 shows that the
283 microbial population density remained relatively unchanged after the addition of NaN₃.
284 This would suggest that the majority of the microbial population contaminating MSW
285 pulp are gram negative bacterial species. This is interesting as the presence of lactic acid
286 contamination is often attributed to the order of gram positive lactic acid bacteria (LAB)
287 (Othman et al., 2017), despite a number of gram negative bacteria, as well as fungal
288 species, also being able to produce lactic acid (Förster and Gescher, 2014; Lin et al.,
289 2018). It was also observed that the hydrolysis supplemented with NaN₃ resulted in the
290 highest glucose recovery, with 10 g/L at 24 hours, which is approximately a 30%
291 improvement over the no antimicrobial control (Figs. 2b and 4b). Whilst NaN₃ is a stable
292 under the reaction conditions, its recalcitrance and toxicity prevent downstream use of
293 the sugar in fermentation processes, so for these applications BIT is preferable.

294 Compared to NaN₃, BIT supplementation resulted in a drastic drop in the total microbial
295 population over the 24 hour time course (Fig. 2a-b). This is not surprising as BIT is
296 described as broad spectrum antimicrobial, possessing bactericidal and fungicidal activity
297 (Silva et al., 2020; Williams, 2006). Interestingly, while no lactic acid was detected in the
298 hydrolysis reaction that had BIT supplementation, glucose titres were not as high as those
299 where NaN₃ was used. Given the significant impact BIT had on microbial population

300 density within the slurry, as well as the absence of any fermentation products, it might
301 suggest that the presence of BIT is hindering glucose formation by other means – perhaps
302 by inhibiting the enzyme activity of the cellulolytic cocktail used for hydrolysis. To test
303 this, we reduced the concentration of BIT supplementation to 0.05% (w/w dry substrate),
304 and found that glucose yield was 10% higher than those hydrolyses supplemented with
305 0.1% (w/w dry substrate) BIT (SI, Fig. S5c). At the lower BIT concentration, final glucose
306 titres after 24 hours were similar to those obtained when NaN_3 was used, with no
307 detectable presence of fermentation products. Persistence of BIT in hydrolysate may
308 pose several issues for further utilisation of sugars, this can be mitigated by neutralisation
309 and distillation steps during downstream processing which decompose BIT into less
310 hazardous molecules (Silva et al., 2020).

311 In contrast to NaN_3 and BIT, neither tetracycline nor hydrogen peroxide was found to be
312 as long lasting in managing the microbial contamination during OFMSW hydrolysis.
313 Hydrogen peroxide is a commonly used disinfectant that works via the oxidation of
314 essential biomolecules, causing damage to proteins, nucleic acids, and lipids (McDonnell,
315 2014). It has been found to be effective against both gram-positive and gram-negative
316 bacteria, fungi, and yeast (McDonnell, 2014). The manual injection of 0.1% (w/w dry
317 substrate) hydrogen peroxide at hour 6 of a hydrolysis reaction resulted in a concomitant
318 rise in dissolved oxygen, however it dropped again to 0 mg/L 2.5 hours later, and
319 remained at 0 mg/L for the remainder of the hydrolysis (Fig. 3c-d). Following the drop in
320 DO at 8.5 hours, the environmental pH also dropped significantly, eventually reaching
321 4.5 by the end of the time course. Between hours 8 to 24 there was a significant
322 accumulation of both lactic acid and acetic acid, explaining this observed drop in
323 environmental pH (Fig. 3c). While the accumulation of acetic acid can be partially

324 explained by the hydrolysis of hemicellulose, the sharp rise in its concentration at hour
325 24 could suggest that some may have been produced microbially as a product of
326 fermentation. These results mirrored well in the analysis of microbial population density
327 over the course of the hydrolysis. An analysis of the number of CFUs showed a drop
328 population density at hour 8, after the addition of hydrogen peroxide, followed by a
329 significant resurgence by hour 24 (Fig. 5). This would suggest that while the addition of
330 hydrogen peroxide had an initial antimicrobial effect, that it was short lived. This agrees
331 with work carried out by Alt et al., 1999, who found that concentrations below 3%
332 hydrogen peroxide were not effective at reducing microbial growth. Hydrogen peroxide
333 is sensitive to self-decomposition, especially at elevated temperatures (Serra-Maia et al.,
334 2018) or by the activity of catalase enzymes which are commonly produced by microbial
335 species. This would suggest that a concentration of 0.1% (w/w dry substrate) of hydrogen
336 peroxide decomposes far too quickly to have long lasting antimicrobial effects. However,
337 we found that while supplementation of concentrations above 0.4% was successful in
338 abolishing microbial contamination, it also dramatically reduced the rate of enzymatic
339 saccharification (SI, Fig. S6), suggesting that an excess of hydrogen peroxide inhibits
340 cellulase activity. However, with the recent discovery that hydrogen peroxide can act as
341 a co-substrate for LPMO enzymes (Müller et al., 2018), it may be the case that a fed batch
342 system where hydrogen peroxide is continuously supplied at a low concentration may
343 have the dual benefit of improving saccharification (via improved LPMO activity) and
344 controlling microbial contamination.

345 Tetracycline is a well-established bacteriostat that exhibits activity against a wide range
346 of microorganisms including gram-positive and gram-negative bacteria, mycoplasmas,
347 rickettsiae, chlamydiae, as well as some eukaryotic parasites (Van Bambeke et al., 2017).

348 It was found that the manual addition of 0.1% (w/w dry substrate) tetracycline once DO
349 dropped to 0 mg/L resulted in the rise and stabilization of DO and environmental pH for
350 approximately 7 hours before DO dropped once again to 0 mg/L at hour 14 (Fig. 3e). An
351 analysis of the number of CFUs at hour 8 showed a significant drop in microbial
352 population density; however, a considerable resurgence in population had occurred by
353 hour 24 (Fig. 5). Despite this, only a small amount of lactic acid (30 mg/L) was detected
354 at this final time point – suggesting the population was skewed towards non-fermenting
355 species. The apparent loss of effectiveness of tetracycline after 7 hours could be attributed
356 to several factors. Tetracycline has been found to be sensitive to both light and high
357 temperatures (López-Peñalver et al., 2010). While the former was not controlled for in
358 this work, the latter is a necessity for effective cellulase enzyme activity (with the reaction
359 temperature being maintained at 50 °C). The necessity for high temperatures during
360 lignocellulosic hydrolysis suggests that this antibiotic is not ideal for these purposes.
361 Furthermore, the use of antibiotics, such as tetracyclines, for the control of microbial
362 populations for non-medical purposes is controversial in the current climate of antibiotics
363 overuse and resistance.

364 Ultimately, the choice of antimicrobial agent will also depend on a number of process
365 specific factors, including the degree and type of microbial contamination of the chosen
366 feedstock, and the eventual fate of the sugar rich hydrolysate (i.e. feedstock for microbial
367 fermentation or chemical conversion).

368 *3.3 Integrated control system with online pH/DO monitoring and automated*
369 *antimicrobial dosing.*

370 With the success of using DO and pH for the early determination of microbial infection,
371 an automated antimicrobial dosing system was developed that could be employed in a
372 production process in order to protect sugar yield and provide a more consistent quality.
373 This automation also has the advantage that experiments can be run overnight
374 unsupervised. The integrated control system developed here involves measuring and
375 logging DO and pH data and using a bespoke algorithm to detect a consistent fall of both
376 metrics. Since DO was found to be an earlier and more useful measure of infection, the
377 algorithm was designed to trigger a pump to deliver a specific dose of anti-microbial agent
378 when the gradient on the DO trace exceeds $-0.028 \text{ mg L}^{-1} \text{ s}^{-1}$ (SI, FigS2). A stand-alone
379 pH measurement was recorded simultaneously. The system was tested without
380 antimicrobial (Fig. 5a), and with NaN_3 alone (Fig. 5b). While NaN_3 was used here to
381 demonstrate the automatic dosing system, the agent can easily be substituted for another
382 (ex. BIT). At the start of the process, the viscosity of the system is high, however after
383 1-2 hours a rheological change was observed (viscosity-break shown by the hatched
384 boxes), and causing fluctuations in the DO reading. Upon detecting a sustained fall in DO
385 at around 5.6 hours, a 10-ml dose of NaN_3 (0.01%, w/w dry substrate) was automatically
386 administered which, over the next hour, resulted in its recovery to pre-infection saturation
387 levels (Fig. 5b). In the control run (Fig 6a), the DO gradient was also plotted during the
388 course of hydrolysis for comparison purposes, even though no automated dosing
389 occurred. A final quantification of glucose at hour 20 revealed that the hydrolysis with no
390 antimicrobial dosing resulted in 10.8 g/L, while the hydrolysis with automatic NaN_3
391 dosing accumulated 17.2 g/L. Automated detection and dosing can improve the process
392 economics, maximise sugar production and improve product consistency.

393 *3.4 Continuous glucose monitoring during enzymatic hydrolysis of MSW pulp*

394 While monitoring of DO and pH provides invaluable information about the state of
395 microbial contamination during the enzymatic hydrolysis of a lignocellulosic feedstock,
396 the purpose of this knowledge is ultimately to use it to maximize sugar yields from the
397 reaction. As such, it is equally valuable to monitor sugar concentration throughout the
398 hydrolysis process (Landari et al., 2018). Currently, these measurements are
399 predominantly carried out offline, using chromatography techniques, such as HPLC, or
400 glucose monitors. While the former technique is time consuming, it benefits from being
401 able to resolve complex sugar mixtures within the slurry, while the latter technique is
402 quicker but specific for only one sugar in the mixture (Leopold et al., 2011). Both
403 techniques tend to be only carried out intermittently throughout the course of the reaction,
404 ultimately resulting in delayed information about total sugar concentration.

405 While *in situ* sugar monitoring using Fournier-Transform Infrared Spectroscopy (FTIR)
406 has been performed previously for sugar quantification in fruit juices and other sugar
407 based products (Landari et al., 2018; Wang et al., 2010), it appears that FTIR has not
408 previously been used for real-time glucose measurement over the course of a
409 lignocellulosic hydrolysis (Sills and Gossett, 2012; Tucker et al., 2001). This is
410 unsurprising given the nature of the slurries involved, which are complex and
411 dynamically changing heterogeneous mixture. In order to achieve a real-time *in-situ*
412 monitoring system for glucose during the enzymatic hydrolysis of MSW pulp, we used
413 FTIR to continuously measure changes in adsorption. A wavenumber of 1035 cm^{-1} was
414 chosen for glucose quantification as it has previously been shown to possess the most
415 linear correlation between absorption and glucose concentration (Nybacka, 2016). An
416 enzymatic hydrolysis was carried out using 7% TS and 5% C-Tec3 (w/w dry substrate),
417 without antimicrobial supplementation. The absorbance readings were converted into

418 glucose concentrations based on a previously created standard curve, (SI, Fig.S3) and
419 compared to periodic samples taken and analysed by HPLC (Fig. 6). Both quantification
420 strategies are tightly correlated, though the glucose concentrations measured by FTIR are
421 consistently higher than those values obtained by HPLC. This is potentially a result of the
422 FTIR method also detecting xylose, cellobiose and other soluble oligomeric sugars.
423 Additionally, intermittent HPLC analysis of glucose plus xylose were also included as
424 an upper threshold. Online FTIR values fit considerably well within those limits, HPLC
425 glucose (below) and HPLC glucose plus xylose (above). This data validates the use of
426 FTIR as an accurate and significantly more rapid method for monomeric sugar
427 determination and has potential to be adopted as a control method within a production
428 process (Blacker et al., 2019).

429 **4. Conclusions**

430 The present study shows that antimicrobial agents are effective in raising MSW sugar
431 hydrolysate titres. BIT and NaN_3 were identified as efficacious antimicrobial agents; the
432 former may be preferred if the sugar is used for fermentations, whilst the latter may be
433 more useful for longer term storage and speciality chemical applications. DO is shown to
434 be a good microbial growth indicator and has been integrated into an operating system
435 for automated mitigation of biological infection in sugar solutions. On-line measurements
436 (pH/DO and FTIR-based glucose monitoring) are useful tools to monitor and control the
437 saccharification process of lignocellulosic feedstocks.

438 **Acknowledgements**

439 The authors would like to thank Fiberight Ltd. for supplying materials and research
440 support, with a special mention to Peter Speller. This work was supported in part by the

441 Innovate UK grants; Driving down the cost of waste derived sugar – CelluPAT (45031-
442 305142), Optimising the production of thermoset resins from MSW-derived sugars –
443 OPTOMS (TS/S003177/1,104391) and the EPSRC Centre for Doctoral Training in
444 Bioenergy grant (EP/L014912/1).

445 **References**

- 446 Alt, E., Leipold, F., Milatovic, D., Lehmann, G., Heinz, S., Schömig, A., 1999.
447 Hydrogen peroxide for prevention of bacterial growth on polymer biomaterials.
448 *Ann. Thorac. Surg.* 68, 2123–2128.
- 449 Bhatia, S.K., Jagtap, S.S., Bedekar, A.A., Bhatia, R.K., Patel, A.K., Pant, D., Rajesh
450 Banu, J., Rao, C. V., Kim, Y.G., Yang, Y.H., 2020. Recent developments in
451 pretreatment technologies on lignocellulosic biomass: Effect of key parameters,
452 technological improvements, and challenges. *Bioresour. Technol.* 300, 122724.
- 453 Blacker, A., Bourne, R., Reynolds, W., 2019. MSW Process Control Systems.
454 WO2019220092.
- 455 Cabrol, L., Quéméneur, M., Misson, B., 2017. Inhibitory effects of sodium azide on
456 microbial growth in experimental resuspension of marine sediment. *J. Microbiol.*
457 *Methods* 133, 62–65.
- 458 Deepak, V., Kalishwaralal, K., Ramkumarpandian, S., Babu, S.V., Senthilkumar, S.R.,
459 Sangiliyandi, G., 2008. Optimization of media composition for Nattokinase
460 production by *Bacillus subtilis* using response surface methodology. *Bioresour.*
461 *Technol.* 99, 8170–8174.
- 462 Du, R., Su, R., Li, X., Tantai, X., Liu, Z., Yang, J., Qi, W., He, Z., 2012. Controlled

463 adsorption of cellulase onto pretreated corncob by pH adjustment. *Cellulose* 19,
464 371–380.

465 Famelart, M.H., Kobilinsky, A., Bouillanne, C., Desmazeaud, M.J., 1987. Influence of
466 temperature, pH and dissolved oxygen on growth of *Brevibacterium linens* in a
467 fermentor. *Appl. Microbiol. Biotechnol.* 25, 442–448.

468 Fenila, F., Shastri, Y., 2016. Optimal control of enzymatic hydrolysis of lignocellulosic
469 biomass. *Resour. Technol.* 2, S96–S104.

470 Förster, A.H., Gescher, J., 2014. Metabolic engineering of *Escherichia coli* for
471 production of mixed-acid fermentation end products. *Front. Bioeng. Biotechnol.* 2,
472 16.

473 Gandla, M.L., Martín, C., Jönsson, L.J., 2018. Analytical Enzymatic Saccharification of
474 Lignocellulosic Biomass for Conversion to Biofuels and Bio-Based Chemicals.
475 *Energies* 11, 2936.

476 Garcia-Ochoa, F., Gomez, E., Santos, V.E., Merchuk, J.C., 2010. Oxygen uptake rate in
477 microbial processes: An overview. *Biochem. Eng. J.* 49, 289–307.

478 Gusakov, A. V., Bulakhov, A.G., Demin, I.N., Sinitsyn, A.P., 2017. Monitoring of
479 reactions catalyzed by lytic polysaccharide monooxygenases using highly-sensitive
480 fluorimetric assay of the oxygen consumption rate. *Carbohydr. Res.* 452, 156–161.

481 Hassan, S.S., Williams, G.A., Jaiswal, A.K., 2018. Emerging technologies for the
482 pretreatment of lignocellulosic biomass. *Bioresour. Technol.* 262, 310–318.

483 Hassen, A., Belguith, K., Jedidi, N., Cherif, A., Cherif, M., Boudabous, A., 2001.
484 Microbial characterization during composting of municipal solid waste. *Bioresour.*

485 Technol. 80, 217–225.

486 Hazar, Y., 2013. Sources for Lignocellulosic Raw Materials for the Production of
487 Ethanol, in: *Lignocellulose Conversion: Enzymatic and Microbial Tools for*
488 *Bioethanol Production*. pp. 21–38.

489 Hendriks, A.T.W.M., Zeeman, G., 2009. Pretreatments to enhance the digestibility of
490 lignocellulosic biomass. *Bioresour. Technol.* 100, 10–18.

491 Islam, M., Toledo, R., Hamdy, M.K., 1999. Stability of virginiamycin and penicillin
492 during alcohol fermentation. *Biomass and Bioenergy* 17, 369–376.

493 Jensen, J.W., Felby, C., Jørgensen, H., Rønsch, G.Ø., Nørholm, N.D., 2010. Enzymatic
494 processing of municipal solid waste. *Waste Manag.* 30, 2497–2503.

495 Johnston, M., 1999. Feasting, fasting and fermenting: Glucose sensing in yeast and
496 other cells. *Trends Genet.* 15, 29–33.

497 Jones, K.O., Williams, D., Montgomery, P.A., Phipps, D., 1992. Dissolved oxygen
498 control in a fermentation of *Saccharomyces cerevisiae* using an automatic tuning
499 PID controller, in: *IFAC Symposia Series*. Publ by Pergamon Press Inc, pp. 247–
500 250.

501 Jönsson, L., Martín, C., 2016. Pretreatment of lignocellulose: Formation of inhibitory
502 by-products and strategies for minimizing their effects. *Bioresour. Technol.* 199,
503 103–112.

504 Landari, H., Roudjane, M., Messaddeq, Y., Miled, A., 2018. Pseudo-continuous flow
505 FTIR system for glucose, fructose and sucrose identification in Mid-IR range.
506 *Micromachines* 9.

507 Leopold, L.F., Leopold, N., Diehl, H.A., Socaciu, C., 2011. Quantification of
508 carbohydrates in fruit juices using FTIR spectroscopy and multivariate analysis.
509 Spectroscopy 26, 93–104. <https://doi.org/10.3233/SPE-2011-0529>

510 Lin, Y.C., Cornell, W.C., Jo, J., Price-Whelan, A., Dietrich, L.E.P., 2018. The
511 pseudomonas aeruginosa complement of lactate dehydrogenases enables use of d -
512 and l -lactate and metabolic cross-feeding. MBio 9.

513 López-Peñalver, J.J., Sánchez-Polo, M., Gómez-Pacheco, C. V., Rivera-Utrilla, J.,
514 2010. Photodegradation of tetracyclines in aqueous solution by using UV and
515 UV/H₂O₂ oxidation processes. J. Chem. Technol. Biotechnol. 85, 1325–1333.

516 McDonnell, G., 2014. The Use of Hydrogen Peroxide for Disinfection and Sterilization
517 Applications, in: PATAI'S Chemistry of Functional Groups. John Wiley & Sons,
518 Ltd, Chichester, UK, pp. 1–34.

519 Meor Hussin, A.S., Collins, S.R.A., Merali, Z., Parker, M.L., Elliston, A., Wellner, N.,
520 Waldron, K.W., 2013. Characterisation of lignocellulosic sugars from municipal
521 solid waste residue. Biomass and Bioenergy 51, 17–25.

522 Mohd-Zaki, Z., Bastidas-Oyanedel, J., Lu, Y., Hoelzle, R., Pratt, S., Slater, F., Batstone,
523 D., 2016. Influence of pH Regulation Mode in Glucose Fermentation on Product
524 Selection and Process Stability. Microorganisms 4, 2.

525 Müller, G., Chylenski, P., Bissaro, B., Eijsink, V.G.H., Horn, S.J., 2018. The impact of
526 hydrogen peroxide supply on LPMO activity and overall saccharification
527 efficiency of a commercial cellulase cocktail. Biotechnol. Biofuels 11, 209.

528 Novozymes, 2012. Novozymes Cellic® CTec3 - Secure your plant's lowest total cost.

529 Novozymes 1–6.

530 Nybacka, L., 2016. FTIR spectroscopy of glucose. Uppsala Universitet.

531 Othman, M., Ariff, A.B., Rios-Solis, L., Halim, M., 2017. Extractive fermentation of
532 lactic acid in lactic acid bacteria cultivation: A review. *Front. Microbiol.*

533 Puri, D.J., Heaven, S., Banks, C., 2013. Improving the performance of enzymes in
534 hydrolysis of high solids paper pulp derived from MSW. *Biotechnol. Biofuels* 6,
535 107.

536 Raspor, P., Goranovič, D., 2008. Biotechnological applications of acetic acid bacteria.
537 *Crit. Rev. Biotechnol.* 28, 101–124.

538 Rich, J.O., Anderson, A.M., Leathers, T.D., Bischoff, K.M., Liu, S., Skory, C.D., 2020.
539 Microbial contamination of commercial corn-based fuel ethanol fermentations.
540 *Bioresour. Technol. Reports* 11, 100433.

541 Riedel, T.E., Berelson, W.M., Neelson, K.H., Finkel, S.E., 2013. Oxygen consumption
542 rates of bacteria under nutrient-limited conditions. *Appl. Environ. Microbiol.* 79,
543 4921–4931.

544 Russo, I., Del Mese, P., Viretto, M., Doronzo, G., Mattiello, L., Trovati, M., Anfossi,
545 G., 2008. Sodium azide, a bacteriostatic preservative contained in commercially
546 available laboratory reagents, influences the responses of human platelets via the
547 cGMP/PKG/VASP pathway. *Clin. Biochem.* 41, 343–349.

548 Schell, D.J., Dowe, N., Ibsen, K.N., Riley, C.J., Ruth, M.F., Lumpkin, R.E., 2007.
549 Contaminant occurrence, identification and control in a pilot-scale corn fiber to
550 ethanol conversion process. *Bioresour. Technol.* 98, 2942–2948.

551 <https://doi.org/10.1016/j.biortech.2006.10.002>

552 Serate, J., Xie, D., Pohlmann, E., Donald, C., Shabani, M., Hinchman, L., Higbee, A.,
553 Mcgee, M., La Reau, A., Klinger, G., Li, S., Myers, C., Boone, C., Bates, D.,
554 Cavalier, D., Eilert, D., Oates, L., Sanford, G., Sato, T., Dale, B., Landick, R.,
555 Piotrowski, J., Ong, R., Zhang, Y., 2015. Controlling microbial contamination
556 during hydrolysis of AFEX-pretreated corn stover and switchgrass: effects on
557 hydrolysate composition, microbial response and fermentation. *Biotechnol.*
558 *Biofuels* 8, 180.

559 Serra-Maia, R., Bellier, M., Chastka, S., Tranhuu, K., Subowo, A., Rimstidt, J.D., Usov,
560 P.M., Morris, A.J., Michel, F.M., 2018. Mechanism and Kinetics of Hydrogen
561 Peroxide Decomposition on Platinum Nanocatalysts. *ACS Appl. Mater. Interfaces*
562 10, 21224–21234.

563 Sills, D.L., Gossett, J.M., 2012. Using FTIR to predict saccharification from enzymatic
564 hydrolysis of alkali-pretreated biomasses. *Biotechnol. Bioeng.* 109, 353–362.

565 Silva, V., Silva, C., Soares, P., Garrido, E.M., Borges, F., Garrido, J., 2020.
566 Isothiazolinone biocides: Chemistry, biological, and toxicity profiles. *Molecules*
567 25.

568 Sluiter, A., Hames, B., Ruiz, R., Scarlata, C., Sluiter, J., Templeton, D., Crocker, D.,
569 2012. Determination of structural carbohydrates and lignin in Biomass. *Lab. Anal.*
570 *Proced.* 17.

571 Tucker, M.P., Nguyen, Q.A., Eddy, F.P., Kadam, K.L., Gedvilas, L.M., Webb, J.D.,
572 2001. Fourier transform infrared quantitative analysis of sugars and lignin in
573 pretreated softwood solid residues, in: *Applied Biochemistry and Biotechnology.*

574 pp. 51–61.

575 Van Bambeke, F., Mingeot-Leclercq, M.-P., Glupczynski, Y., Tulkens, P.M., 2017.

576 Mechanisms of Action, in: Infectious Diseases. Elsevier, pp. 1162-1180.e1.

577 Van Dyk, J.S., Pletschke, B.I., 2012. A review of lignocellulose bioconversion using

578 enzymatic hydrolysis and synergistic cooperation between enzymes-Factors

579 affecting enzymes, conversion and synergy. *Biotechnol. Adv.*

580 Wahlström, R.M., Suurnäkki, A., 2015. Enzymatic hydrolysis of lignocellulosic

581 polysaccharides in the presence of ionic liquids. *Green Chem.* 17, 694–714.

582 Wang, J., Kliks, M.M., Jun, S., Jackson, M., Li, Q.X., 2010. Rapid Analysis of Glucose,

583 Fructose, Sucrose, and Maltose in Honeys from Different Geographic Regions

584 using Fourier Transform Infrared Spectroscopy and Multivariate Analysis. *J. Food*

585 *Sci.* 75, C208–C214.

586 Ward, B., 2014. Bacterial Energy Metabolism, in: *Molecular Medical Microbiology:*

587 *Second Edition.* Elsevier Ltd, pp. 201–233.

588 Williams, T.M., 2006. The mechanism of action of isothiazolone biocides, in: *NACE -*

589 *International Corrosion Conference Series.* NACE International, pp. 060901–

590 0609017.

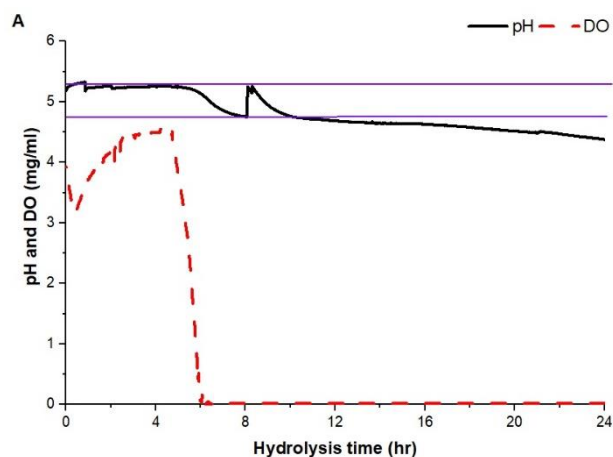
591

592

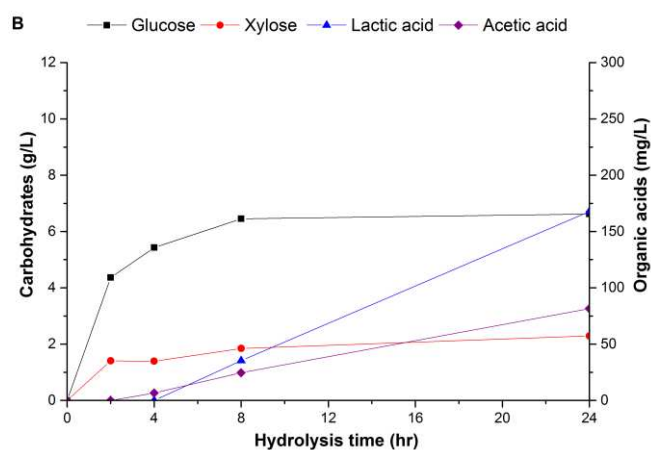
593

594

595



600



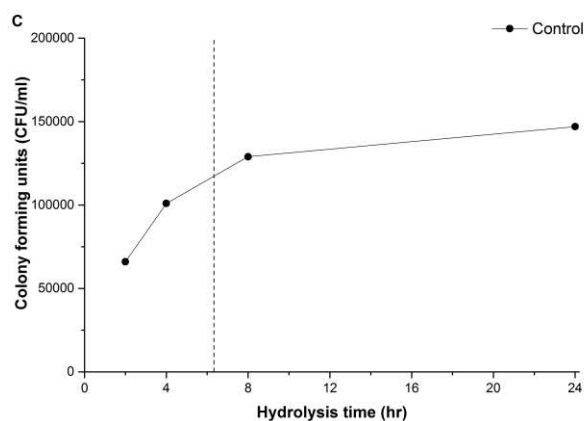
601

602

603

604

605



606

607

608

609

610

611 **Figure 1.** Monitoring of (a) pH and DO, (b) carbohydrates/organic acids, (c) and
612 microbial population density (CFU/ml) over the course of a 24 hour enzymatic hydrolysis
613 of 6% MSW pulp using 2% C-Tec3 (w/w dry substrate) with no antimicrobial
614 supplementation. No pre-sterilization of pulp or equipment was performed. Hydrolysis

615 was carried out at 50 °C, with pH initially set to 5.25, and readjusted at hour 8. Purple
616 lines (Fig. 1a) represent the optimum pH-range (4.75-5.25) for the Cellic[®] CTec3 enzyme
617 cocktail (Novozymes, 2012) and dashed line (Fig 2c) the timing when DO reached 0 mg/L
618 and anti-microbial was dosed.

619

620

621

622

623

624

625

626

627

628

629

630

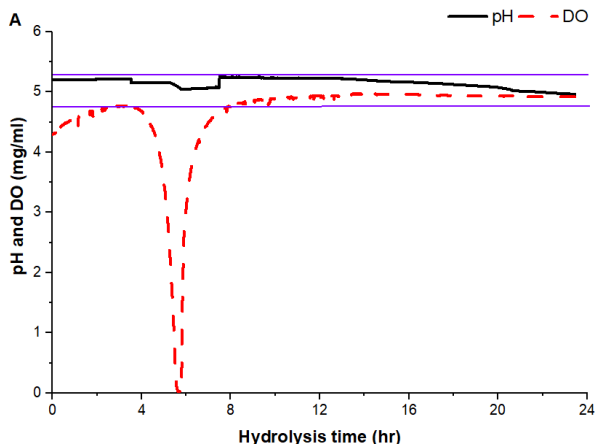
631

632

633

634

635



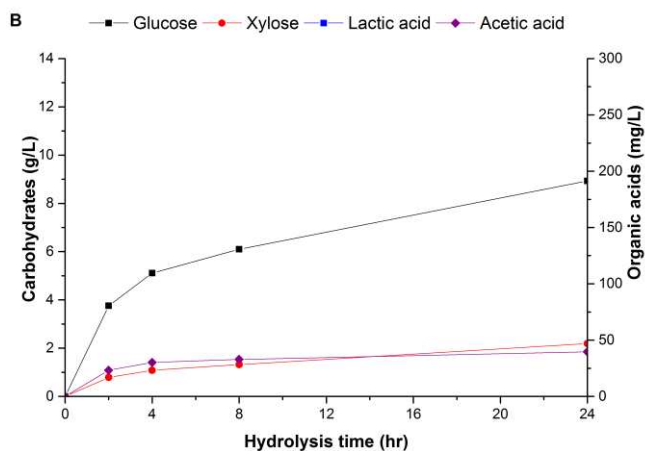
636

637

638

639

640



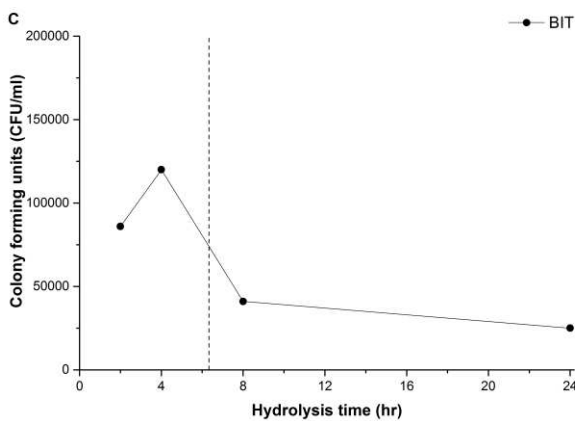
641

642

643

644

645



646

647

648

649

650

651 **Figure 2.** Monitoring of (a) DO and pH, (b) saccharification/fermentation products, and
652 (c) microbial population density (CFU/ml) over the course of a 24 hour enzymatic
653 hydrolysis of 6% MSW pulp using 2% C-Tec3 (w/w dry substrate), where 0.1% BIT (w/w
654 dry substrate) was supplemented into the slurry once DO reached 0 mg/L. No pre-

655 sterilization of pulp or equipment was performed. Hydrolysis was carried out at 50 °C,
656 with pH initially set to 5.25, and readjusted at hour 8. Purple lines (Fig. 1a) represent the
657 optimum pH-range (4.75-5.25) for the Cellic[®] CTec3 enzyme cocktail (Novozymes,
658 2012) and dashed line (Fig 2c) the timing when DO reached 0 mg/L (anti-microbial
659 dosing).

660

661

662

663

664

665

666

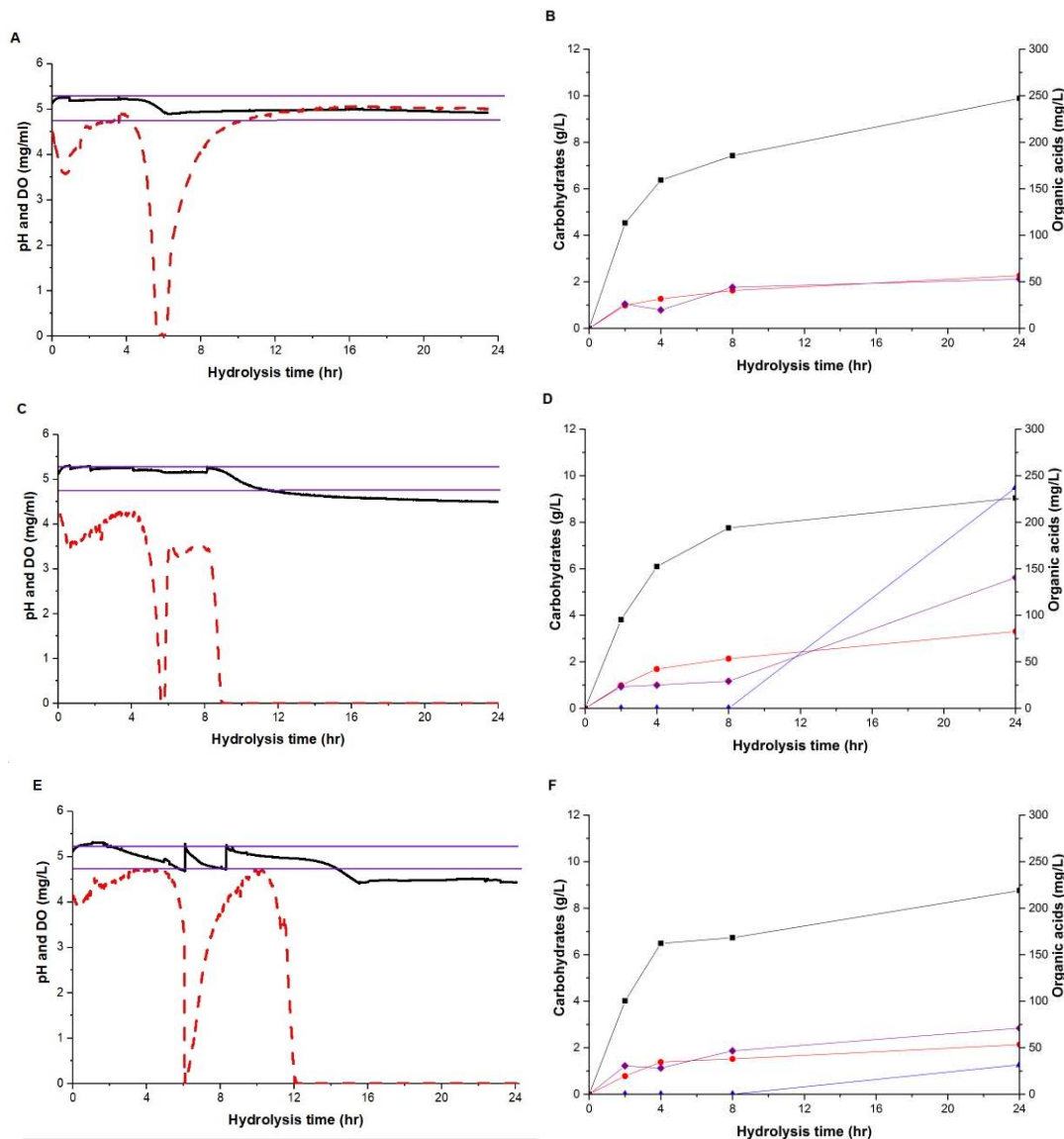
667

668

669

670

671



672 **Figure 3.** Evaluation of the efficiency of several antimicrobial agents for controlling
673 microbial population during the enzymatic hydrolysis of 6% MSW pulp using 2% C-Tec3
674 (w/w dry substrate). Graphs on the left pH and DO, graphs on the right carbohydrate and
675 organic acid concentrations. Manual antimicrobial dosing of 0.1% (w/w dry substrate)
676 occurred once DO reached 0 mg/L, with (a,b) sodium azide, (c,d) hydrogen peroxide, and
677 (e,f) tetracycline. Purple lines (Figs 4a,c,e) represent the optimal pH-range (4.75-5.25)
678 for Cellic[®] CTec3 enzymes (Novozymes, 2012)

679

680

681

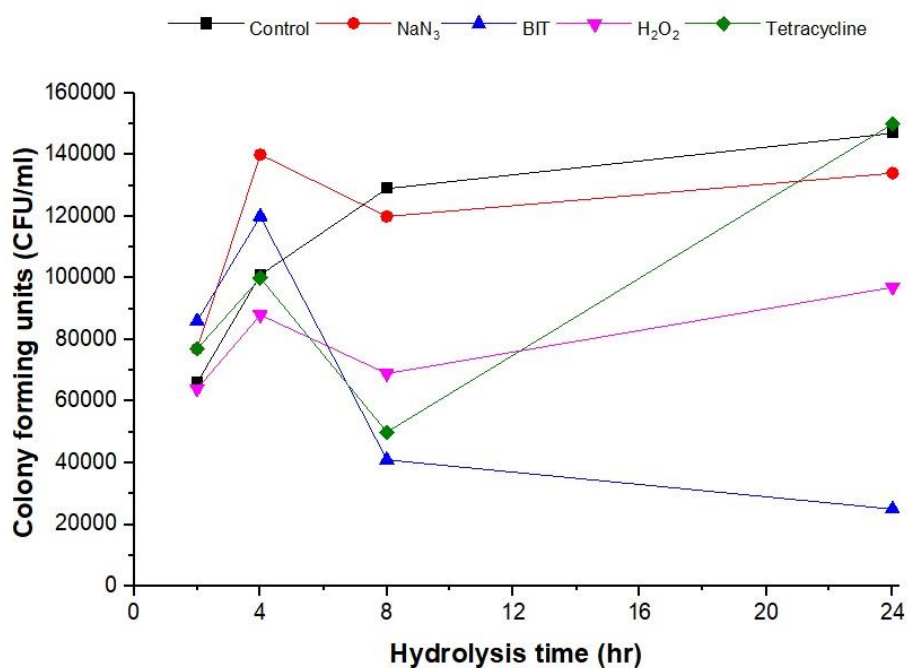
682

683

684

685

686



687

688

689

690

691

692

Figure 4. Number of colony forming units (CFU) per millilitre of slurry detected at 2, 4, 8, and 24 hours from 6% MSW hydrolyses where either 0.1% (w/w dry substrate) BIT, sodium azide, hydrogen peroxide, tetracycline, or no antimicrobial was supplemented into the reaction mixture at approximately hour 6. A serial dilution of slurry at each time point was plated onto LB agar and incubated at 50 °C for 16 hours before quantification.

693

694

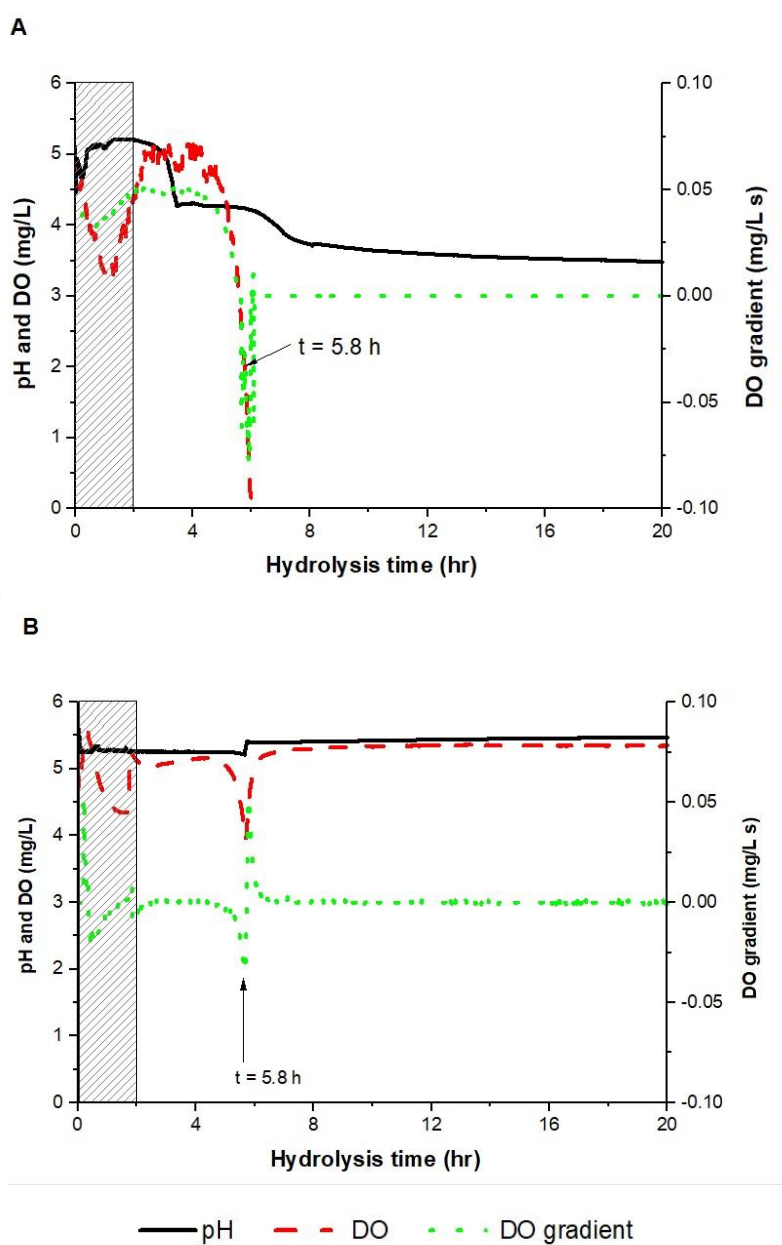
695

696

697

698

699



700

701

702

703

704

705

706

707 **Figure 5.** Process monitoring of pH and DO using automated antimicrobial dosing: (a)

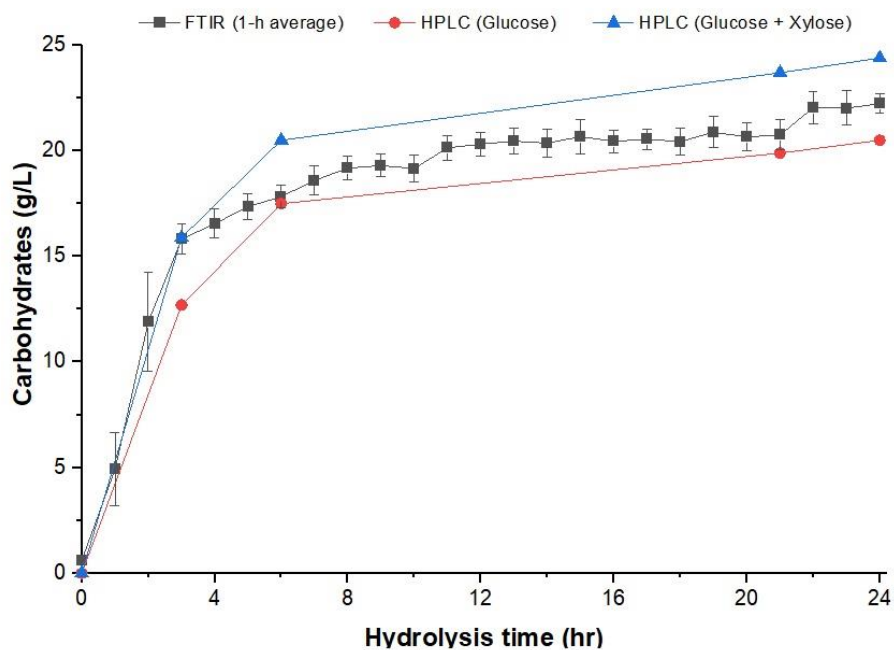
708 control, (b) 0.01% (w/w of dry substrate) NaN₃. Reactions were carried out at 8% TS and

709 2% E:S. The 30 s readings are plotted as trend-lines, hatched-boxes represent the

710 “viscosity break” and arrows the timing when the DO gradient was $-0.028 \text{ mg L}^{-1} \text{ s}^{-1}$.

711 Final glucose concentrations (t = 20h) were 10.8, 17.2 for the control and NaN₃.

712 Experiments were carried out in duplicate with standard deviations



720 **Figure 6.** Comparison of continuous FTIR measurement (1-hr averages) and intermittent
 721 off-line HPLC measurements (glucose and glucose plus xylose) for the quantification of
 722 monomeric sugars during the enzymatic hydrolysis of 7% MSW pulp with 5% C-Tec3
 723 and no antimicrobial supplementation. FTIR values represent the average \pm standard
 724 deviation of each measurement taken over the course of an hour.